

# First Order Kaon Condensation in Neutron Stars: Finite Size Effects in the Mixed Phase

Travis Norsen<sup>1</sup> and Sanjay Reddy<sup>2</sup>

<sup>1</sup>*Dept. of Physics, University of Washington, Seattle, WA 98195*

<sup>2</sup>*Institute for Nuclear Theory, University of Washington, Seattle, WA 98195*

(November 5, 2018)

## Abstract

We study the role of Coulomb and surface effects on the phase transition from dense nuclear matter to a mixed phase of nuclear and kaon-condensed matter. We calculate corrections to the bulk calculation of the equation of state (EOS) and the critical density for the transition by solving explicitly for spherical, cylindrical and planar structures. The importance of Debye screening in the determination of the charged particle profiles is studied in some detail. We find that the surface and Coulomb contributions to the energy density are small but that they play an important role in the determination of the critical pressure for the transition, as well as affecting the size and geometry of favored structures. This changes the EOS over a wide range of pressure and consequently increases the maximum mass by  $\sim 0.1 M_{\odot}$ . Implications for transport properties of the mixed phase are also discussed.

arXiv:nucl-th/0010075v1 23 Oct 2000

## I. INTRODUCTION

It is now universally thought that some type of phase transition will occur in nuclear matter at high densities. In particular, a transition to de-confined quark matter must occur at sufficiently high density. There may also exist a transition to pion or kaon condensed matter at intermediate densities. In any of these cases, the phase transition is expected to soften the equation of state (EOS) and thereby affect the mass-radius relation of neutron stars, favoring lower maximum masses and smaller radii compared to neutron stars containing only nucleon degrees of freedom. Phase transitions can also influence transport properties and weak interaction rates, which in turn affect various potentially observable features of neutron star evolution such as its cooling history, spin down rates, glitches and related phenomena.

A generic feature of first order phase transitions in neutron star matter is that a mixed phase region, where the nuclear phase coexists with a denser and energetically favorable new phase, is mechanically stable and can thereby occupy a significant spatial region in the interior of a neutron star [1]. The best studied example of a first order transition at high baryon density is the quark-hadron phase transition, where model calculations indicate that the mixed phase is favored for a wide range of pressure and consequently can occupy a large spatial extent in the neutron star interior (2-6 km).

In a recent article, Glendenning and Schaffner studied a model for kaon condensation, where the transition to the kaon condensed phase is first order [3]. Thus, unlike earlier studies of kaon condensation [4,5], where the transition was second order, the model due to Glendenning and Schaffner predicts a mixed phase where the kaon phase coexists with a nuclear phase. This naturally leads to the question of how surface and coulomb effects will influence the extent and structure of the mixed phase. Earlier studies, in the context of a quark-hadron phase transition, showed that surface and Coulomb effects are important [2]. It was found that the range of pressures over which the mixed phase is favored depended sensitively on the (poorly known) surface tension between the nuclear and quark phase [2].

In the present work, we calculate surface and Coulomb contributions (including the effects of Debye screening) to the thermodynamic potential in a mixed phase containing kaons. We identify their importance in the determination of the equation of state, the size and dimensionality of spatial structures, and the critical density for the onset of the mixed phase.

We begin by describing the model for a first order kaon condensate in §2. After a critical review of the standard procedure for dealing with finite size effects, the surface and coulomb contributions to the Gibbs potential are evaluated in §3. §4 addresses the changes induced by inclusion of Debye screening of electrons. In §5, we discuss the implications of our findings to the structure of neutron stars and transport properties in the mixed phase region. We summarize our main findings, and discuss their implications in §6.

## II. FIRST ORDER KAON CONDENSATION

In this section we briefly review the model proposed by Glendenning and Schaffner [3] which predicts a first order transition from the nuclear to the kaon condensed phase. The nuclear phase is described by a relativistic, Walecka type, field theoretical model including

the isovector meson  $\rho$  as well as cubic and quadratic self-interactions of the scalar meson [10,9]. The Lagrangian for the nucleon sector is given by

$$\begin{aligned}\mathcal{L}_N = & \bar{\Psi}_N \left( i\gamma^\mu \partial_\mu - m_N^* - g_{\omega N} \gamma^\mu V_\mu - g_{\rho N} \gamma^\mu \vec{\tau}_N \cdot \vec{R}_\mu \right) \Psi_N \\ & + \frac{1}{2} \partial_\mu \sigma \partial^\mu \sigma - \frac{1}{2} m_\sigma^2 \sigma^2 - U(\sigma) - \frac{1}{4} V_{\mu\nu} V^{\mu\nu} \\ & + \frac{1}{2} m_\omega^2 V_\mu V^\mu - \frac{1}{4} \vec{R}_{\mu\nu} \cdot \vec{R}^{\mu\nu} + \frac{1}{2} m_\rho^2 \vec{R}_\mu \cdot \vec{R}^\mu,\end{aligned}\quad (1)$$

where  $m_N^* = m_N - g_{\sigma N} \sigma$  is the nucleon effective mass, which is reduced compared to the free nucleon mass due to the scalar field  $\sigma$ . The vector fields corresponding to the omega and rho mesons are given by  $V_{\mu\nu} = \partial_\mu V_\nu - \partial_\nu V_\mu$ , and  $\vec{R}_{\mu\nu} = \partial_\mu \vec{R}_\nu - \partial_\nu \vec{R}_\mu$  respectively. The scalar self-interaction term is given by  $U(\sigma) = (1/3)bm_N(g_{\sigma N}\sigma)^3 + (1/4)c(g_{\sigma N}\sigma)^4$ , where  $b$  and  $c$  are dimensionless coupling constants.  $\Psi_N$  is the nucleon field operator with  $\vec{\tau}_N$  the nucleon isospin operator. The five coupling constant,  $g_{\sigma N}$ ,  $g_{\omega N}$ ,  $g_{\rho N}$ ,  $b$ , and  $c$ , are chosen to reproduce the empirical properties of nuclear matter at saturation density [10].

Kaons are included in the model in the same fashion as the nucleons, by coupling to the  $\sigma$ ,  $\omega$  and  $\rho$  meson fields. There exist in the literature several meson-exchange Lagrangians which attempt to describe kaon-nucleon interactions. A detailed discussion of these models and their relation to the Chiral Lagrangian proposed by Kaplan and Nelson [4] can be found in Pons, et al. [6]. In the present paper we employ the Lagrangian proposed by Glendenning and Schaffner. The kaon Lagrangian is given by

$$\mathcal{L}_K = \mathcal{D}_\mu^* K^* \mathcal{D}^\mu K - m_K^* K^* K, \quad (2)$$

where  $K$  denotes the isospin doublet kaon field. The covariant derivative  $\mathcal{D}_\mu = \partial_\mu + ig_{\omega K} V_\mu + ig_{\rho K} \vec{\tau}_K \cdot \vec{R}_\mu$  couples the kaon field to the vector mesons and the kaon effective mass term  $m_K^* = m_K - g_{\sigma K} \sigma$  describes its coupling to the scalar meson.  $\vec{\tau}_K$  is the kaon isospin operator. The vector coupling constants are determined by isospin and quark counting rules [3], and are given by  $g_{\omega K} = g_{\omega N}/3$  and  $g_{\rho K} = g_{\rho N}$ . The scalar coupling is fixed by fitting to an empirically determined kaon optical potential in nuclear matter. Albeit poorly known, the real part of the optical potential in nuclear matter as deduced from kaonic atoms indicates that  $80 \text{ MeV} \lesssim U_K(n_o) \lesssim 180 \text{ MeV}$  [7,8]. Here, we choose  $U_K(n_o) = 120 \text{ MeV}$  to fix  $g_{\sigma K}$ . Lower values of the optical potential favor a second order transition, while higher values make the first order transition stronger. For the purpose of this study, we require that the phase transition be first order but the qualitative features of the results found here are independent of its precise value.

In the mean-field approximation only the time component of the vector fields and the isospin 3-component of the isovector field can have nonzero mean values. The equations of motion (EOM) for the non-strange meson fields can be derived from the above Lagrangians and are given by

$$-\nabla^2 \sigma + m_\sigma^2 \sigma = -\frac{dU}{d\sigma} + g_{\sigma B}(\rho_n^s + \rho_p^s) + g_{\sigma k} f_\pi^2 \theta^2 m_k^*, \quad (3)$$

$$-\nabla^2 \omega + m_\omega^2 \omega = g_\omega(\rho_n + \rho_p) - g_{\omega K} f_\pi^2 \theta^2 (\mu_K + X), \quad (4)$$

$$-\nabla^2 r + m_\rho^2 r = g_\rho(\rho_p - \rho_n) - g_{\rho K} f_\pi^2 \theta^2 (\mu_K + X). \quad (5)$$

where the meson fields  $\sigma, \omega, r$  now represent the appropriate mean values,  $X = g_{\omega K}\omega + g_{\rho K}r$ , and  $\rho_{(n,p)}^{(s)}$  are the (scalar) densities of neutrons and protons. The ansatz  $K = f_K\theta/\sqrt{2}$  has been made, where  $f_K$  is the kaon decay constant and  $\theta$  is a dimensionless kaon field strength parameter. In the bulk approximation, the gradient terms are omitted and the EOM become non-linear algebraic equations to be solved self-consistently for the meson fields. The EOM for the kaon is

$$\left(\mathcal{D}_\mu\mathcal{D}^\mu + m_K^{*2}\right) K = 0. \quad (6)$$

where  $m_K^* = m_K - g_{\sigma K}\sigma$  is the kaon effective mass and  $\mu_K^* = \mu_e + X$ . In terms of  $\theta$ , the kaon EOM is re-expressed as

$$\nabla^2\theta = \left(m_K^{*2} - \mu_K^{*2}\right)\theta. \quad (7)$$

In the bulk mean field calculation, the solution to Eq.(7) and the other meson field equations are obtained with the gradient terms set equal to zero. This determines the condensate amplitude and the expectation values of the other meson fields [3] and completely specifies the ground state of matter at the mean field level. However, surface effects are ignored since the gradient terms in the EOM are neglected. In this work we explicitly retain the gradient term and solve Eq.(7) for the kaon condensate in the Wigner-Seitz approximation using spherical, cylindrical, or planar geometry as appropriate. This is described in detail in §3.

The energy density of the nuclear phase is

$$\begin{aligned} \epsilon_N = & \int_0^{k_{F_n}} \frac{d^3k}{(2\pi)^3} \sqrt{k^2 + m_N^{*2}} + \int_0^{k_{F_p}} \frac{d^3k}{(2\pi)^3} \sqrt{k^2 + m_N^{*2}} + \frac{\mu_e^4}{4\pi^2} \\ & + \frac{1}{2} \left( (\nabla\sigma)^2 + m_\sigma^2\sigma^2 \right) + \frac{1}{2} \left( (\nabla\omega)^2 + m_\omega^2\omega^2 \right) + \frac{1}{2} \left( (\nabla r)^2 + m_\rho^2 r^2 \right) + U(\sigma) \end{aligned} \quad (8)$$

where  $k_F^{(n,p)}$  are the neutron and proton Fermi momenta and  $\sigma, \omega$  and  $\rho$  are the expectation values of the meson fields in the absence of kaons (note the gradient terms are zero in the bulk calculation and are included here for completeness). In the phase containing kaons, the meson field equations are modified and consequently their expectation values will change. Therefore, the energy density in the kaon phase due to the nucleon is given by Eq. (8), but with different expectation values for  $\sigma, \omega$  and  $\rho$  meson fields. The contribution to the energy density from the kaon field itself is

$$\epsilon_{\text{kaon}} = \frac{1}{2} f_K^2 \left[ (\nabla\theta)^2 + (m_K^*)^2\theta^2 \right]. \quad (9)$$

In the absence of gradient terms the kaons do not directly contribute to the pressure as they form an s-wave condensate. However, as is well known, the attractive interaction between nucleons and kaons lowers the nuclear contribution to the pressure, which is given by

$$\begin{aligned} p = & \frac{1}{3\pi^2} \int_0^{k_{F_n}} \frac{k^4 dk}{\sqrt{k^2 + m_N^{*2}}} + \frac{1}{3\pi^2} \int_0^{k_{F_p}} \frac{k^4 dk}{\sqrt{k^2 + m_N^{*2}}} + \frac{\mu_e^4}{12\pi^2} \\ & + \frac{1}{2} \left( (m_\omega\omega)^2 + (m_\rho\rho)^2 - (m_\sigma\sigma)^2 \right) - U(\sigma) \end{aligned} \quad (10)$$

where the meson mean field values are affected by the presence of a kaon condensate.

### III. SURFACE AND COULOMB EFFECTS IN THE MIXED PHASE

A complete description of the mixed phase should include surface and Coulomb contributions to the energy density. The Coulomb energy arises because each of the two phases is electrically charged. If the electric charge densities were small, the size of energetically favored structures would be very large, and the contribution of the surface tension to the overall energy density would become vanishingly small. In our case, however, the electric charge densities are large (comparable to the baryon number densities), resulting in small structures (5-7 fm) for which the surface to volume ratio is large. Consequently the surface tension makes an important contribution to the total energy density.

Unlike in the quark-hadron transition, where the surface tension is poorly known, the surface tension between the kaon and nucleon phases can be calculated within the purview of the model described earlier because the two phases (and hence also the surface between them) are considered within the same theoretical framework. Before detailing the procedure we adopt in this work, we will briefly review the methodology often employed in calculating surface and Coulomb contributions to the thermodynamics.

#### A. Critique of the Bulk Calculation

The bulk calculation (what we refer to as the “bulk calculation” is defined below) of droplet phase thermodynamics, especially in the context of the mixed phase containing nuclei and dripped neutrons, is described in detail in several earlier works [11,12]. In a recent work, Christiansen, *et al.* [13] have studied the kaon-nucleon mixed phase using similar methods. The bulk calculation proceeds as follows: At a given baryon chemical potential, the electron chemical potential is adjusted so as to obtain equal pressures in the two phases. This determines the composition of each phase, allowing one to calculate the volume fraction of each phase based on the requirement of global electric charge neutrality. The various thermodynamic quantities are then determined by volume-fraction-weighted averaging.

The bulk energy density (Eq. 8) is supplemented with the inclusion of surface and Coulomb terms. The surface tension coefficient  $\sigma_0$  is estimated by computing the interface energy between two semi-infinite slabs by explicitly including the gradient terms, as was done for the nuclear-kaon phase boundary in Ref. [13]. Once the surface tension is known, the surface contribution to the energy density for a structure of size  $R$  and Wigner-Seitz radius  $R_{WS}$  can be approximated by

$$\epsilon_{Surface} = \frac{\chi\sigma_0 d}{R} \quad (11)$$

where  $\chi = (R/R_{WS})^d$  is the volume fraction of the kaon phase and  $d$  is the dimensionality ( $d = 3$  for droplets,  $d = 2$  for cylinders, and  $d = 1$  for slabs). The Coulomb energy is

$$\epsilon_{Coulomb} = 2\pi(\Delta\rho)^2 r^2 \chi f_d(\chi) \quad (12)$$

where

$$f_d(\chi) = \frac{2/(d-2)(1 - \frac{1}{2}d\chi^{1-2/d}) + \chi}{d+2}, \quad (13)$$

$\Delta\rho$  is the difference in electric charge densities of the two phases, and  $\chi$  is the volume fraction of the rare phase [11].

The total energy density is then given by

$$\epsilon = \chi\epsilon_K + (1 - \chi)\epsilon_N + \epsilon_{Surface} + \epsilon_{Coulomb}. \quad (14)$$

The stable size for geometrical structures is found by minimizing this energy density with respect to variations in the size  $R$ . In the usual method, this procedure assumes that the two bulk energy densities  $\epsilon_N$  and  $\epsilon_K$  do not vary with  $R$ , so that the minimization amounts to making the sum of surface and Coulomb contributions as small as possible. As is well-known, this calculation establishes that the favored size is that which permits  $E_{Surface} = 2E_{Coulomb}$  independent of the dimension [11].

The bulk calculation is premised on: (1) pressure equilibrium between the two phases; (2) constancy of the bulk energy densities (and surface tension) as the structure size varies; (3) the neglect of the finite thickness of the phase boundary; and (4) the neglect of modifications to the charged particle distributions due to electrostatic forces (Debye screening). In what follows we address each of these assumptions and show that none of them are valid for the case in study.

First, the assumption of pressure equality cannot hold in general. To see this, assume we have a system that has separated into two phases, with the total energy given by  $E = E_1 + E_2 + E_{Surface}$ , where  $E_{1(2)}$  refers to the energy in phase 1(2). If the surface tension is not a strong function of the shape of the phase boundary, the surface energy will be given by  $E_{Surface} = \sigma A$  where  $A$  is the area of the boundary. In equilibrium, the total energy will be minimized with respect to the volume occupied by phase 1,  $V_1$ . (The boundary will move and thereby change the volumes occupied by the two phases until the total energy is minimized.) Differentiating the expression for the total energy with respect to  $V_1$  and setting the result to zero gives

$$p_1 - p_2 = \sigma \frac{dA}{dV_1}, \quad (15)$$

where  $p_1 = -\partial E_1/\partial V_1$  and  $p_2 = -\partial E_2/\partial V_2$  are the pressures in the two phases, which are seen to differ by an amount proportional to the surface tension and the derivative of the boundary area with respect to the volume of the rare phase. For the case of slabs, the indicated derivative is zero since the boundary can move back and forth without changing its area. For the case of spherical droplets and cylindrical rods, however, the derivative is proportional to  $R^{-1}$  and the pressure difference between the two phases may become large for small structures. The pressure, however, is tied to the other thermodynamic quantities through the usual relation  $\epsilon - \sum \mu n = -p$ . Consequently, the bulk energy density, baryon number density and the chemical potentials cannot remain constant; they change as the size is varied due to changes in the pressure of the kaon phase. Note that a change in the bulk properties of the kaon phase for small structures also necessitates a change in the surface tension, which depends on the integrated gradients between the two phases.

For small structures the finite thickness of the surface region also plays an important role. The thickness of the boundary layer between the two phases is of order 5 fm. For structures

of about this size, only a very small region at the center obtains the bulk value of the kaon field, that is, the gradient terms in the meson fields are non-zero nearly everywhere in the kaon structure. Thus, for small structures, the assumption of zero boundary thickness grossly overestimates the extent of the bulk kaon region. Any attempt to produce a structure with a radius *smaller* than this thickness will result in dramatic changes to the bulk properties of the rare phase, since the fields don't have room to achieve their usual bulk values at the center of the droplet. Therefore, the bulk approximation completely breaks down for structures smaller than this size.

Thus assumptions (1-3) of the bulk calculation can only be trusted in the limit of relatively large structures. In order to quantify this statement, we have constructed a sequence of kaon-condensate droplets, by explicitly solving the kaon EOM, having different radii and at a fixed external pressure. Various thermodynamic quantities are then calculated and compared to results obtained in the bulk calculation.

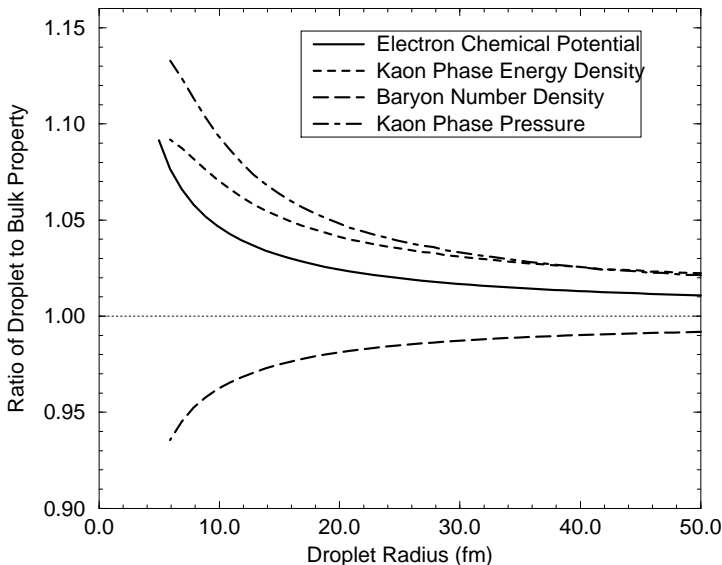


FIG. 1. Ratio of droplet properties to corresponding bulk properties as a function of droplet radius. The droplets are constructed with the external pressure (pressure in the nuclear phase) held fixed at a value  $p = .35\text{fm}^{-4}$ .

Fig. 1 shows the ratio of droplet properties to bulk-calculation properties as a function of droplet size. As expected, the quantities asymptote to their bulk values in the limit of large droplets, but differ from their bulk values at the 10% level for droplets with radii below about 10 fm. This behavior is typical of small structures, being more pronounced for droplets, less so for rods and is absent for slabs (for the pressure equilibrium reasons discussed previously). These finite size effects are therefore likely to play an important role in the vicinity of the critical density associated with onset of the mixed phase where the favored structures are droplets. Here, it is important to note that finite size corrections tend to increase the kaon phase energy density and decrease the baryon number density with decreasing radius. This is significant because both of these effects tend to make small droplets energetically less favorable than predicted by the bulk calculation. Also, the increase of the electron chemical

potential for small structures near the critical density acts to make the electric charge density of the nuclear phase negative, making it impossible to satisfy the charge neutrality condition, except in the case of unreasonably large structures. Both of these effects suggest that the critical pressure for the transition may be increased from its naive bulk value. This is indeed what we find.

Thus, the first three assumptions above are valid only in the limit of large structures. Assumption (4), however, is known to be valid only for structures smaller than the smallest Debye screening length. (Note that in the previous analysis we neglected screening.) The typical Debye screening length of electrons at the density of interest here is 7-10 fm [2]. For larger droplets the charged particle distributions will readjust to screen the droplet charge. To demonstrate this, we show the particle density profiles for a droplet with fixed total number of kaons, for the two cases: with and without screening included in the equations of motion. To include this effect, we use a relaxation procedure in which we start with an initial guess for the shape of the electric potential in the Wigner-Seitz cell, solve for the kaon EOM to obtain the charged particle profiles, and then recalculate the electric potential using the new profiles. This is then repeated until convergence.

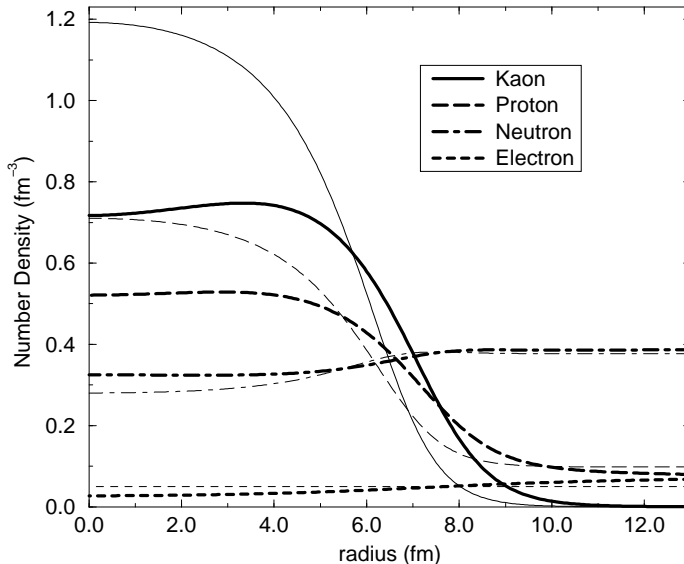


FIG. 2. Comparison of droplet profiles with and without electron Debye screening. The screened droplet (thick lines) and the unscreened droplet (thin lines) each contain a total kaon number of 1100. The effect of screening is to push many of the kaons near the surface of the droplet and thus greatly reduce the central kaon number density. A similar effect occurs for electrons, although the overall densities are lower. The neutron profile is changed only slightly by screening, while the proton density closely follows the changes in the kaon distribution.

The effect of the electrostatic forces on the particle density profiles is shown in Fig. 2. The large negative potential at the center of the droplet tends to push the negatively charged kaons toward the surface region, and the electrons out beyond the surface. The proton distribution follows more closely the changes in the kaon distribution since the strong interaction between the kaons and protons overwhelms the Coulomb effect. Screening becomes more



pronounced for droplet radii larger than typical Debye screening length, which in the present case appears to be about 5 fm. Droplets larger than this size are greatly deformed, with the kaons residing mainly on the surface.

Although this deformation increases the energy density associated with the strong interactions by forcing the fields to take on less than ideal values in the central regions, the overall effect is to significantly reduce the Coulomb energy of the structures. This is essentially as expected. After all, allowing the fields to rearrange themselves in accordance with the electric potential is tantamount to adding a degree of freedom to the system; so it is no surprise that the net effect is for the system to find a way to lower its total energy.

While the deformation due to Debye screening indeed becomes less important for smaller structures, it appears to never become negligible. This is also expected, since the screening length is approximately the same size as the boundary thickness and it is not possible for structures to become smaller than this thickness without being greatly deformed. The quantitative effects of screening on the energetics and geometry of structures will be discussed further in §4. For now, suffice it to say that one cannot expect *a priori* the effects of Debye screening to be small compared to other finite size effects.

To summarize, the assumptions of the bulk calculation are inconsistent. Some are valid only in the limit of very large structures, while the neglect of screening is plausible only in the opposite limit. Consequently, a description of the mixed phase calls for a more careful treatment. This is main goal of this work. In the what follows we describe the procedure we adopt to calculate the thermodynamics of the mixed phase.

## B. Energy Minimization and Results

Our task here is to determine the ground state configuration of a local region of a neutron star interior at a specified pressure. Consequently, the appropriate thermodynamic potential is  $G = E + pV$ , the Gibbs potential. With conservation of baryon number, the ground state will minimize the Gibbs potential per baryon:

$$g = \frac{G}{N_B} = \frac{E + pV}{N_B} = \frac{\epsilon + p}{n_B}. \quad (16)$$

Here  $\epsilon$  is the energy density,  $p$  is the pressure, and  $n_B$  is the baryon number density. Global electrical neutrality is imposed by considering the energy density and baryon number density averaged across a Wigner-Seitz cell containing zero net charge.

The Gibbs free energy per baryon in the kaon mixed phase, computed in the bulk approximation is shown in Fig.3. The results shown do not include the the surface and Coulomb contributions. The Gibbs energy of the homogeneous phase containing only nucleons is also shown (solid line). The critical pressure for the onset of the mixed phase is determined by the requirement that the pressure in the two phases be equal, phases be oppositely charged and the Gibbs energy be lower than that of the homogeneous nucleon phase. From the figure we see that this occurs at a pressure  $p = 0.28 \text{ fm}^{-4}$ , corresponding to a baryon number density of  $n_B = 0.43 \text{ fm}^{-3}$ .

The goal of the present work is to identify the changes that result to this simple picture when finite-size effects are correctly incorporated. In order to include surface and Coulomb contributions, we solve the kaon EOM. We begin with a small value of the kaon field at a

finite radius, and then integrate back toward the origin. The chemical potentials are then adjusted until the desired pressure is reached and the kaon field attains zero slope at the origin. The different geometries (spheres vs. cylinders vs. slabs) are implemented by using the appropriate form of the Laplacian operator for that geometry. We omit the effect of Debye screening in what follows; it will be discussed in detail in the next section. The Wigner-Seitz cell size is determined as usual by the requirement of overall charge neutrality.

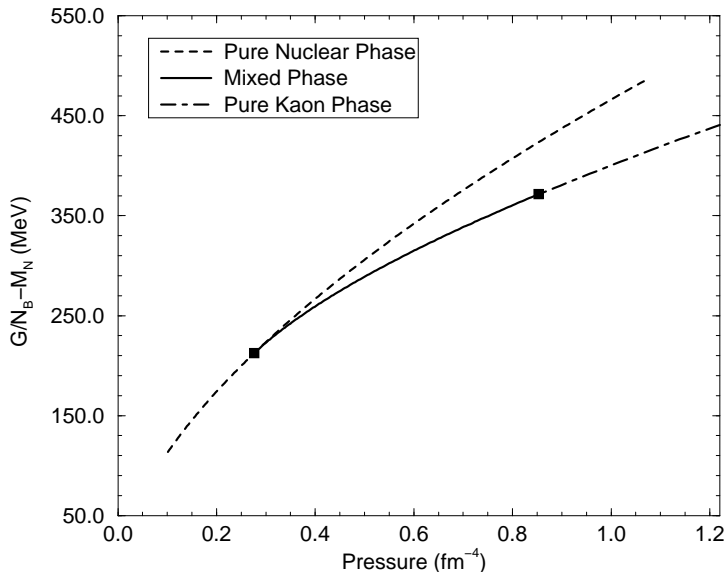


FIG. 3. Gibbs energy per baryon as a function of pressure for the pure nucleon phase and the kaon mixed phase. The mixed phase is clearly energetically favored over the entire pressure range of its existence, indicated by the two squares. However, the values shown here ignore surface and Coulomb contributions to the energy as well as Debye screening.

The energy density is calculated as in Eq. 8 with the gradient terms included. This allows for exact treatment of the energy associated with the surface and obviates the need to compute the surface tension and curvature coefficients. The Coulomb energy density is  $\epsilon_{Coulomb} = \frac{\epsilon_0}{2} |E(r)|^2$  where  $E$  is the electric field determined from Gauss' law for the relevant geometry by explicitly integrating the electric charge density up to a given radius. At a given pressure, the most stable configuration will minimize the Gibbs free energy per baryon, as described above. We construct a sequence of droplets/rods/slabs of varying size and study how  $G/N_B$  varies with  $R$  at fixed pressure. The results are qualitatively as expected. For large structures, the Coulomb energy dominates, while for very small structures the surface energy dominates. At intermediate sizes there is a trade-off which results in a minimum of  $G/N_B$  vs.  $R$ . This minimum determines the ground state at a given pressure.

Some details of this minimization deserve mention. Because of the variation of the electron chemical potential with structure size, the nucleonic matter outside of the kaon condensate structure sometimes becomes negatively charged for small structures. This occurs for pressures just above the bulk critical pressure, where the bulk approximation predicts a nucleonic phase with small positive charge. If both phases become negatively charged, however, no Wigner-Seitz cell can be defined, and the structure in question is ruled out. Thus

the requirement of overall electric charge neutrality forbids the existence of reasonably-sized structures at pressures just above the bulk critical pressure.

The Gibbs energy per baryon is plotted as a function of pressure for the three different geometries in Fig. 4. Note that the values are shown relative to the Gibbs energy of the pure nuclear phase. As expected, there is a smooth transition between the relative favorability of drops (which are preferred at lower pressures) to rods and slabs as the pressure is increased. Although we do not construct them explicitly here, this sequence is expected to continue in the usual way through anti-rods and anti-drops in which the nuclear phase becomes the rare phase. The significant feature of our result is the comparison of the structures to the Gibbs energy per baryon of electrically neutral pure nucleon matter. Just above the critical pressure, where droplets are the favored geometry and therefore will be present according to the bulk calculation, we find that the Gibbs energy is lower in the nucleonic phase than in the mixed phase. This remains the case over a wide range of pressures, until droplets finally become favorable relative to pure nuclear matter at a pressure about 50% higher than the bulk calculation value of the critical pressure, nearly  $.40 \text{ fm}^{-4}$  instead of  $.28 \text{ fm}^{-4}$ . At a slightly higher pressure, rods and subsequently slabs take over as the energetically favored geometry.

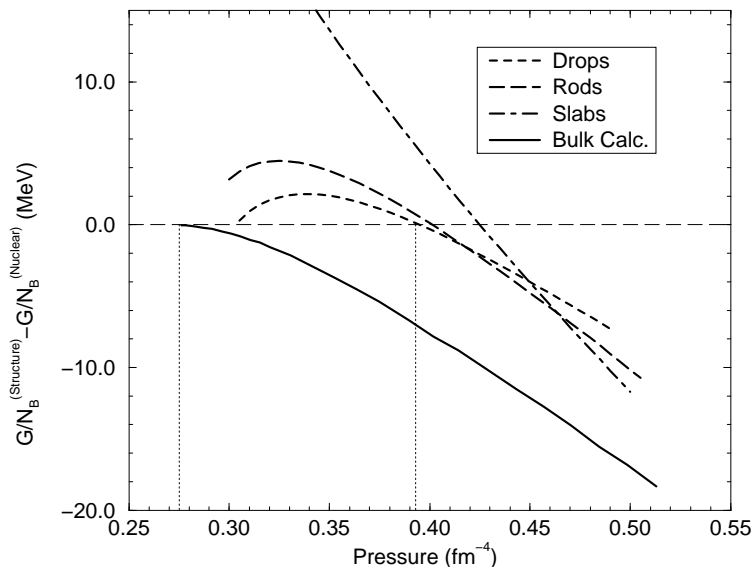


FIG. 4. Gibbs energy per baryon as a function of pressure for droplets, rods, and slabs. The energy is measured relative to the Gibbs energy per baryon of pure nuclear matter at the same pressure; hence, a given geometric structure is favored only when it lies below zero. The bulk calculation (neglecting surface and Coulomb effects) is included for comparison. Note the change in value of the critical pressure (i.e., the pressure marking the onset of a mixed phase), indicated here by two vertical lines for the old and new values. Note also that these results omit the effects of Debye screening, which will be discussed shortly.

The reason for the curvature in the droplet and rod energy at low pressures involves electric charge neutrality, as discussed previously. At these low pressures, the variation of the structure size necessitates a change in the electro-chemical potential. This change then

results in the nucleonic matter outside the kaon region becoming less and less positively charged. At some minimum size, the matter outside becomes uncharged, and the Wigner-Seitz radius becomes infinite and the kaon filling fraction goes to zero. In general, as the structure size is reduced at constant pressure, the kaon phase volume fraction approaches zero, and the Gibbs energy approaches (from above) its value for pure electrically neutral nucleonic matter at the same pressure. So although the mixed phase energy appears to come close to the pure nucleon phase values near the bulk critical pressure, a mixed phase is never in fact favored at these low pressures.

The striking result that we find here is the significant increase in the critical pressure at which the mixed phase becomes favorable. Qualitatively, this increase in the critical pressure should be expected since the bulk calculation neglected the surface and Coulomb energies. An increase in the critical pressure will make the equation of state stiffer over this range and correspondingly the maximum mass of the neutron star will increase. In addition, the radial extent of the mixed phase in the interior will be significantly reduced.

#### IV. DEBYE SCREENING

The effect of Debye screening on the radial dependence of the particle densities was shown in Fig. [2]. Charged particle profiles had to readjust quite significantly to lower the coulomb energy. Clearly, the effect of the deformation of particle profiles caused by screening is to increase the hadronic part of the energy density associated with the structure. This must occur because the fields no longer take on their optimal values over a sizable region of the structure. The net effect of screening, however, is to lower the total energy, since the reduction in the Coulomb energy due to screening is larger than the cost in hadronic energy associated with the deformation.

The qualitative effects of screening on the Gibbs energy are shown in Fig. [5]. The results illustrate the importance of the Coulomb energy relative to other contributions. For example, the differences in Gibbs energies among unscreened droplets of different sizes are small compared to the differences between unscreened droplet and screened droplets of any size. Screening also results in a qualitative change in the radius dependence of the Gibbs free energy. The Gibbs free energy of the screened droplets decreases with increasing radius for small to intermediate size droplets.

How are the results of the previous section affected by screening? To answer this, we must first point out another qualitative effect of screening which again involves electrical charge neutrality. As shown in Fig. [2], Coulomb forces tend to repel the negatively charged electrons away from the kaon droplet. Whenever the Wigner-Seitz radius is large (which can happen either when the kaon structure itself is large, or when the kaon filling fraction is low) this repulsion results in an over-abundance of electrons in the region outside of the kaon structure. But as before, once the electric charge density of the nucleonic phase becomes negative, it is no longer possible to define a Wigner-Seitz cell, and the structure under consideration is forbidden.

We find that precisely this problem occurs for all droplets below a pressure of about  $p = .35 \text{ fm}^{-4}$ . Above this pressure, where it is possible to construct a fully screened globally electrically neutral droplet, the Gibbs energy per baryon is indeed lowered somewhat from the values plotted in Fig. [4]. This results in the critical pressure decreasing slightly from

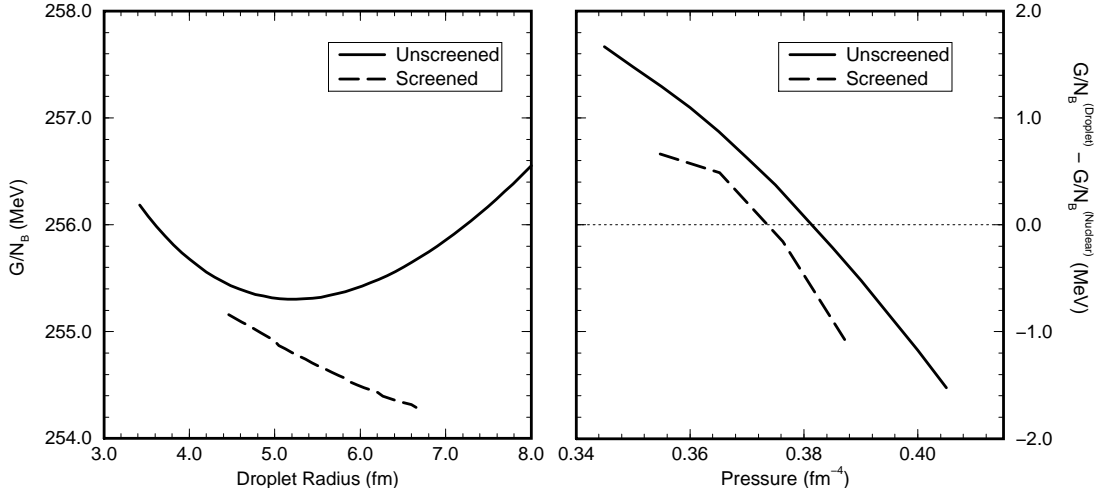


FIG. 5. Gibbs energy per baryon as a function of droplet radius, for different amounts of screening. The screening is controlled by shifting the electrochemical potential at each radius by a fraction of the true electric potential. By turning on the screening slowly, one clearly sees the qualitative effect of the overall energy per baryon being lowered due to the reduction in Coulomb energy.

the new value quoted earlier, but the change here is small. The first fully screened structure we can produce with Gibbs energy per baryon below that of the pure nucleonic phase occurs at a pressure of  $.375 \text{ fm}^{-4}$  (compare this with the critical pressure  $\sim 0.385 \text{ fm}^{-4}$  when Debye screening was ignored). Thus, while the Debye screening can have large effects on the particle density profiles, it has a relatively small effect on the free energy density (less than one MeV per baryon), as can be seen in the right panel of Fig. 5. Consequently the results of the previous section remain qualitatively unchanged: the inclusion of finite-size effects significantly increases the critical pressure for transition to a mixed phase.

Because the changes in Coulomb energy associated with screening are large compared to the energy differences between various geometries at a given pressure, screening will also play a dominant role in the determination of structures that are preferred at a given pressure. The qualitative feature of droplets being replaced by rods (and subsequently slabs) as the pressure is increased is expected to remain. But the particular pressures at which the transition from one geometry to the next occurs may vary from the picture of Fig. [4]. Thus, if one is only interested in the long wavelength thermodynamic properties of the system, it is safe to ignore Debye screening. However, to describe the mixed phase in more detail, i.e., specify the particle profiles and the geometries that are favored at a given pressure Debye screening must be accounted for.

## V. NEUTRON STAR PROPERTIES

### A. Structure

The equation of state determines the neutron star structure through the Tolman-Oppenheimer-Volkov (TOV) equation:

$$\frac{dp}{dr} = -\frac{[p(r) + \epsilon(r)][M(r) + 4\pi r^3 p(r)]}{r(r - 2M(r))} \quad (17)$$

where  $p$  is the pressure,  $\epsilon$  is the energy density, and

$$M(r) = 4\pi \int_0^r \epsilon(r)r^2 dr \quad (18)$$

is the total mass enclosed at radius  $r$ . The solution to the TOV equation are shown in Fig. 6 for three cases: pure nuclear matter, the bulk calculation of the mixed phase, and a calculation of the mixed phase as described in this work which properly accounts for surface and coulomb energy. The left panel of the figure shows the variation of the total gravitational mass as a function of the central pressure. We find that the maximum neutron star mass is increased by about  $0.1M_\odot$  relative to the bulk calculation of the mixed phase. This is as expected since the critical pressure for the transition was shown to increase due to the finite size effects. The distribution of mass and internal composition of the star for a given value of the central pressure are shown in the right panel. The dashed lines show results for the case where finite size effects are included; this is to be contrasted with the results obtained in the bulk approximation shown by the solid curve. The spatial extent of the mixed phase region is also influenced by finite size effects. The extent of the mixed phase region in the inner core is shown for both cases and indicates that the finite size effects cause the mixed phase region to shrink. It must however be noted that we are comparing the structure of stars with different gravitational mass but the same central pressure.

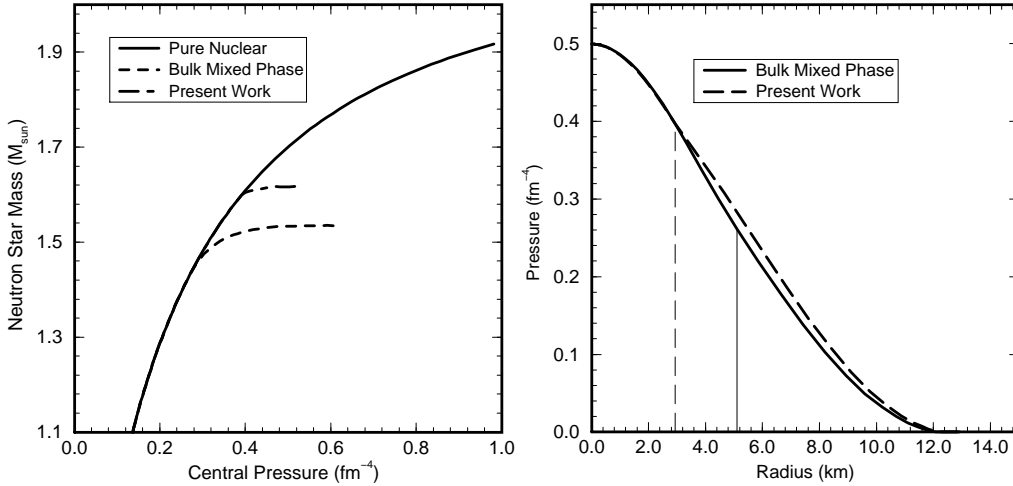


FIG. 6. Mass as a function of the central pressure for a pure nuclear equation of state, the bulk mixed calculation without finite-size effects, and the realistic calculation of the present work. A correct treatment of surface and Coulomb energies increases the critical pressure for the realization of the mixed phase, and the neutron star maximum mass by  $\sim 0.1M_\odot$ . The right panel compares the internal structure of a star with and without finite size corrections included in a description of the mixed phase. The vertical lines indicate the outer edge of the mixed phase for the two descriptions.

## B. Transport Phenomena

Transport properties in a mixed phase can differ greatly from those of uniform matter since the mixed phase allows for new processes that cannot occur in a translationally invariant system. Finite size effects play a central role in the determination of the transport characteristics of a heterogenous phase since they depend sensitively on the composition, size and geometry of the structures present. In what follows we briefly discuss a few examples of transport process which are strongly influenced by the finite size effects.

In a recent article, it was shown that low energy neutrinos couple coherently to the droplet structures and consequently the neutrino mean free path in a mixed phase was greatly reduced [15]. The neutrino scattering rate depends on the total weak charge, and on the filling fraction. The cross section for the coherent neutrino-droplet scattering varies as the square of the total weak charge. Thus, the neglect of screening effects alone, which could overestimate the weak charge in a droplet by as much as 30 – 50 % (see Fig.5), could result in a mean free path estimate that was smaller by 50 – 75 %. Furthermore, coulomb correlations between droplets decreases the net neutrino scattering rate when the  $E_\nu \lesssim 1/d$ , where  $d = 2R_{WS}$  is the inter-droplet spacing. Again, an accurate description of finite size and Debye screening effects is required to calculate the neutrino mean free path in the mixed phase [15]. The filling fraction of the kaon phase, denoted by  $\chi$ , at a pressure  $p = 0.40 \text{ fm}^{-4}$  in the bulk approximation is  $\chi_{bulk} = 0.23$  while the more detailed treatment yields  $\chi = 0.13$ . Again, this substantial change is due to the increase of the electron chemical potential for small droplets.

The results of this work will also influence calculations of the melting temperature of the lattice of droplets. This becomes obvious when we note that the electric charge distributions are strongly modified. In addition, our findings here affect the location and the nature of the interface between the solid-mixed phase and the liquid-nuclear phase. The physics of this interface has been shown to play an important role in damping r-mode instabilities in cold and rapidly rotating neutron stars [16]. In general, since the transport characteristics depend primarily on the size and distance between structures, this calls for a detailed description of the mixed phase wherein screening and finite surface effects are incorporated. In particular, studies of the early evolution of neutron stars [17], where neutrino transport plays an important will be strongly influenced by finite size effects discussed here.

## VI. CONCLUSIONS AND DISCUSSION

The earliest papers on first-order kaon condensation in neutron stars ignored finite size effects such as surface and Coulomb energies. Since then, these effects have been introduced into calculations by assuming that certain quantities remain fixed as the physical size of geometric structures is varied. By explicitly constructing these structures, however, we have shown these assumptions to be unwarranted. In particular, the energy densities, number densities, and chemical potentials vary at the 10% level as the size is reduced toward the boundary thickness. These changes in the bulk properties of the two phases preclude the possibility of determining the most stable structures by minimizing only the surface and Coulomb contributions to the energy. By including these effects correctly, we find that the critical pressure for the onset of the mixed phase is increased dramatically, with the further

consequence that the maximum neutron star mass is increased back toward its value for the pure nuclear equation of state.

Clearly, we have not accounted for all finite size effects that arise in the mixed phase. We examine some assumptions of our work here and comment on corrections omitted. The calculations presented here were based on the Thomas-Fermi approximation for the nucleon fields, which we expect to be valid based on our observation that the average nucleon density is large compared to the size of the density gradients [14]. The Wigner-Seitz approximation could in principle introduce corrections to the filling fraction. However, we expect these corrections to be most important at large filling fraction where the Wigner-Seitz description is accurate because the favored geometry is planar. In addition a careful treatment of the nucleon fields would introduce shell effects that may be important for small structures. These effects have been neglected here since we expect their contributions to the Gibbs potential to be small (typically, we expect that  $\delta E_{shell} \sim A^{1/6}$  compared to  $A^1$  or  $A^{2/3}$  dependence of volume and surface contributions, where  $A$  is the total baryon number of the droplet).

The increase in the critical pressure will also reduce the radial extent of the mixed phase. This will potentially affect our pictures of neutrino transport, glitches, r-mode instabilities, and other issues involved in neutron star structure and viscosity calculations. Additionally, as pointed out by Heiselberg, Pethick and Staubo [2], the mixed phase may not be realized in practice if the nucleation time is too large, even if the mixed phase is energetically favored. Our work here gives a hint in that direction: correct inclusion of surface and Coulomb energies dramatically reduces the energetic favorability of the mixed phase over a wide range of pressures. This increase in energy, however, necessarily applies not only to the stable structures of 5 – 6 fm, but also to the smaller transitional structures which must be passed through in the process of nucleation. In short, our work suggests that the energy barrier to nucleation may be somewhat higher than previously thought, resulting in an increase of the expected time required for the phase transition to occur.

The apparent experimental observation of relatively high-mass neutron stars (e.g., Ref. [18–20]) has been cited as evidence that kaon condensation does not occur in neutron stars. We hypothesize a different interpretation which appears to be consistent with these high-mass observations. A sufficiently heavy proto-neutron star (PNS) may undergo a kaon-condensate phase transition due to thermal nucleation while it is still relatively hot. This will of course soften the equation of state and perhaps lead to gravitational collapse of a massive PNS to a black hole [21]. In contrast, a PNS which is insufficiently massive, on the other hand, will not achieve the critical density for kaon-condensation and will therefore cool in the standard way. If it subsequently acquires mass through accretion the low temperature may preclude the possibility of forming a kaon-condensed mixed phase, even if the central pressure exceeds the critical pressure for the transition. The energy barrier to nucleation via quantum tunneling would simply be too high, and the neutron star could exist in a metastable state for a long time. This (for now hypothetical) scenario would explain how the observation of high-mass neutron stars (in excess of the maximum mass allowed by the kaon mixed-phase equation of state) may not contradict the existence of kaon condensation; these high-mass stars would need only to have acquired a part of their mass through accretion after cooling, which appears in fact to be likely. In any case, further examination of the time scale for nucleation of kaon-condensate droplets is clearly interesting and warrants further work.



Finally, it should be pointed out that the relevance of these issues is not restricted to the case of kaon condensation only. Any first-order phase transition that occurs in neutron stars will share the same qualitative properties. Hence, it is reasonable to suggest that a correct inclusion of finite size effects in the deconfinement transition will have similar results to the ones we have shown here, i.e., an increase in the critical pressure and a possible increase in the nucleation time allowing for metastability.

## **Acknowledgements**

We thank George Bertsch, Wick Haxton and Eduardo Fraga for useful discussions. This work is supported in part by National Science Foundation Graduate Research Fellowship (TN) and the US department of Energy grant DE-FG03-00-ER41132 (SR).

## REFERENCES

- [1] N. K. Glendenning, Phys. Rev. D **46**, (1992) 1274
- [2] H. Heiselberg, C. J. Pethick, and E. F. Staubo, Phys. Rev. Lett. **70**, (1993) 1355
- [3] N. K. Glendenning, and J. Schaffner-Bielich, Phys. Rev. Lett. **81**, (1998) 4564  
N. K. Glendenning, and J. Schaffner-Bielich, Phys. Rev. C **60**, (1999) 025803
- [4] D. Kaplan and A. Nelson, Phys. Lett. **175B**, (1986) 57
- [5] V. Thorsson, M. Prakash, and J. M. Lattimer, Nucl. Phys. **A572**, (1994) 693
- [6] J. A. Pons, S. Reddy, P. Ellis, M. Prakash, and J. M. Lattimer Phys. Rev. C **62**, (2000) 035803
- [7] E. Friedman, A. Gal, and C. J. Batty, Nucl. Phys. **A579**, (1994) 578
- [8] A. Ramos and E. Oset, Nucl. Phys. **A671**, (2000) 481
- [9] N. K. Glendenning, *Compact Stars, Nuclear Physics, Particle Physics and General Relativity*, (Springer-Verlag, New York, 1997)
- [10] B. Serot and J. D. Walecka, *Advances in Nucl. Physics*, **16**, edited by J. W. Negele and E. Vogt (Plenum, New York, 1986)
- [11] D. G. Ravenhall, C. J. Pethick and J. R. Wilson Phys. Rev. Lett. **50**, (1983) 2066
- [12] C. J. Pethick and D. G. Ravenhall, Annu. Rev. Nucl. Part. Sci. **45**, (1995), 429
- [13] M. Christiansen, N. K. Glendenning, and J. Schaffner-Bielich, Phys. Rev. C **62**, (2000) 025804
- [14] W. D. Myers and W. J. Swiatecki, Ann. Phys. (NY) **55**, (1969) 395
- [15] S. Reddy, G. F. Bertsch, and M. Prakash, Phys. Lett. **475B**, (2000) 1
- [16] L. Bildsten and G. Ushomirsky, Astrophys. Jl. **529**, (2000) L33
- [17] J. A. Pons, J. A. Miralles, M. Prakash, and J. M. Lattimer, astro-ph/0008389
- [18] W. Zhang, T.E. Strohmayer, and J.H. Swank, Astrophys. Jl. **482**, (1997) L167
- [19] M.H. van Kerkwijk, astro-ph/0001077
- [20] Jerome A. Orosz and Erik Kuulkers, astro-ph/9901177
- [21] M. Prakash, I. Bombaci, M. Prakash, P. J. Ellis, P. J. Ellis, J. M. Lattimer and R. Knorren, Phys. Rep. **280**, (1997) 1